Stability Analysis of Carbon/Epoxy Plate with the use of Finite Elements Method

Hélio de Assis Pegado[1], Bruna Mara Alves da Silva[2]

[1]*Dept. of Mechanical Engineering, Federal University of Minas Gerais*
Antonio Carlos Avenue, 6627, 31270-901, Belo Horizonte, MG, Brazil
helio@demec.ufmg.br
[2]*Dept. of Mechanical Engineering, Federal University of Minas Gerais*
Antonio Carlos Avenue, 6627, 31270-901, Belo Horizonte, MG, Brazil
bruna.mara16@gmail.com

Abstract. The Laminated plates subjected to in-plane compressive loads are studied in this research, taking into account laminate different configurations and boundary conditions. The critical buckling load for these configurations is calculated using a commercial Finite Elements Program. The mesh convergence is tested, and the 60x60 mesh is chosen because their results are very close to the classical references, and the time of execution is lower than sixty seconds. The Finite Element Program is performed and the results obtained show a good agreement with the literature, which demonstrate the validity of the model adopted. The critical buckling load and its mode are evaluated, and the influence of several boundary conditions and the fiber directions are studied. The results obtained are discussed, and the influence of the different design parameters of the laminate on static stability is verified.

Keywords: buckling, static stability, composite laminate

1 Introduction

The aircraft, rockets, missiles and other aerospace structures are composed of panels, i.e., plates and shells. These panels under compression and/or shear loads can buckle when the load reach a critical value. This critical load was obtained for many different isotropic structures subjected to various loads and the results are available in several books and papers.

The composite materials are materials made up of layers of fibers aligned in a certain direction and a matrix that is designed to hold out the loading. These materials are very light in relation to the metals that have the same strength and stiffness. Moreover, the engineers can customize the material and the structure to support certain loadings. The aeronautical industry disseminated your use beginning in the helicopters and gliders and after in the commercial aircraft, as shown in the Fig. 1.

The buckling of the plate is studied in several classic books [1],[2] and [3]. The buckling can be studied by means of partial fourth-order differential, and the equations can be solved using analytical methods to certain boundary conditions. However, the approach more employed is to solve using approximate methods as Galerkin, Ritz and Finite Element Method. Several books studied the behavior of the composite structures when the plate is subjected to critical loads [4],[5],[6] and [7].

This work shows the stability analysis of composite plate subjected to axial compressive load. The Von Karman equation are discretized using the Finite Element Method and the elements of the commercial software NASTRAN is used. The influence of the boundary conditions and the direction of the fibers about the stability border is studied. The results are presented in Tables and Figures according to the number of layers, the critical load and the fiber angle.

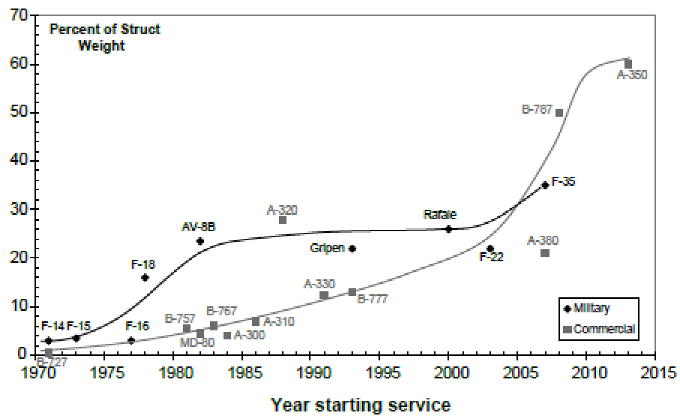

Figure 1. Applications of Composites in military and civilian aircraft structures[5]

2 Modelling the Problem

2.1 Fundamental Assumptions

The main assumptions are that the model satisfies the Classical Theory of Lamination and the Kirchhoff Hypothesis for plates. These hypotheses [7] can be summarized in: each ply is quasi-homogeneous and orthotropic; the laminated is thin, and its lateral dimensions are much larger than its thickness and is loaded only in-plane (plane stress condition); the deflections of the mid-surface are small compared to the thickness of the plate, and the slope of the deflected plate is small; the mid-plane is unstrained when the plate is subjected to pure bending; and the plane sections normal to the mid-plane remain normal to the mid-plane after bending.

2.2 Laminated Matrix

The laminated equation is obtained using strain-displacements relations considering the plane x-y coincides with the mid-plane. The derivation of the stress-strain relation for each ply and the laminated equation obtainment is available in the literature.

The plate loaded by compressive forces per length unit N_x, N_y and shear forces N_{xy} and the resultant moments per length unit M_x, M_y and M_{xy} can be related to its deformation by a matrix - eq.(1), where the superscript 0 represents the mid-surface strains.

$$\begin{Bmatrix} N_x \\ N_y \\ N_{xy} \\ M_x \\ M_y \\ M_{xy} \end{Bmatrix} = \begin{bmatrix} A_{11} & A_{12} & A_{16} & B_{11} & B_{12} & B_{16} \\ A_{21} & A_{22} & A_{26} & B_{12} & B_{22} & B_{26} \\ A_{16} & A_{26} & A_{66} & B_{16} & B_{26} & B_{66} \\ B_{11} & B_{12} & B_{16} & D_{11} & D_{12} & D_{16} \\ B_{21} & B_{22} & B_{26} & D_{12} & D_{22} & D_{26} \\ B_{16} & B_{26} & B_{66} & D_{16} & D_{26} & D_{66} \end{bmatrix} \cdot \begin{Bmatrix} \epsilon_x^0 \\ \epsilon_y^0 \\ \gamma_{xy} \\ \kappa_x \\ \kappa_y \\ \kappa_{xy} \end{Bmatrix} \tag{1}$$

Where the A_{ij} is the stretching stiffness coefficient, the D_{ij} is the bending stiffness coefficient and the B_{ij} indicate the coupling coefficient which are calculated using eq. (2), (3) and (4). The superscript N is the number of layers, the subscript k is the k-th layer, z_k is the distance between the k-th layer and the reference, and the $[Q_{ij}]$ is the matrix that presents the influence of the lamination angle. As the laminated plate is symmetric then all $B_{ij} = 0$.

$$[A_{ij}] = \sum_{i=1}^{N} [Q_{ij}]_k (z_k - z_{k-1}) \tag{2}$$

$$[B_{ij}] = \frac{1}{2}\sum_{i=1}^{N}[Q_{ij}]_k(z_k^2 - z_{k-1}^2) \tag{3}$$

$$[D_{ij}] = \frac{1}{3}\sum_{i=1}^{N}[Q_{ij}]_k(z_k^3 - z_{k-1}^3) \tag{4}$$

2.3 Von Karman Equation

The equation of motion can be obtained using Newton's Second Law or Energy Method. For plate bending, static analysis and symmetric laminate, the equation is simplified and it is shown in Narita and Leissa [8] - eq. (5).

$$D_{11}\frac{\partial^4 w}{\partial x^4}+4D_{16}\frac{\partial^4 w}{\partial x^3\partial y}+2(D_{12}+2D_{66})\frac{\partial^4 w}{\partial x^2\partial y^2}+4D_{26}\frac{\partial^4 w}{\partial x\partial y^3}+D_{22}\frac{\partial^4 w}{\partial y^4} = N_x\frac{\partial^2 w}{\partial x^2}+N_y\frac{\partial^2 w}{\partial y^2}+2N_{xy}\frac{\partial^2 w}{\partial x\partial y} \tag{5}$$

This equation is normalized using adimensional parameter: the effects of N_x are represented by $\lambda = \frac{-N_x a^2}{D_0}$ where $D_0 = \frac{E_1 h^3}{12(1-\nu_{12}\nu_{21})}$ and h is the laminated thickness.

2.4 Numerical Model

This research uses the Nastran Software to analyse the composite plate. The 2D orthotropic material (MAT8) and property laminated thin plates (PCOMP) are employed in the construction of the finite element model. This property defines a laminate following the classical lamination theory. Each unidirectional ply, its thickness, their material properties and its lamination angle is described in this property card. The software evaluates the matrices [A], [B] and [D], as presented in the previous section.

As described in the Nastran's Guide [9], the model solves the static stability using the Linear Bifurcation Analysis (LBA). The global matrix stiffness used in buckling analysis is the linear matrix stiffness - $[k_a]$ plus the differential stiffness matrix - $[k_d]$: $[k] = [k_a] + [k_d]$. The Guide shows that as the critical load is evaluated. U represents the potential energy and u_i the displacement of the i-th degree of freedom in the eq.(6).

$$[U] = 0.5\{u\}^T[k_a]\{u\} + 0.5\{u\}^T[k_d]\{u\}$$

$$\frac{\partial U}{\partial u_i} = [k_a]\{u\} + [k_d]\{u\}$$

$$[[k_a] + \lambda_i[k_d]]\{u\} = 0 \tag{6}$$

The critical load is obtained: $P_{crit} = \lambda_i.P_a$ where P_a is the applied load in the plate.

2.5 Convergence Test

The finite element method was used to discretize the differential equation, eq. 5, and the five mesh results are shown in Tab. 1.

Several combinations of meshes and fibers angles are studied and the results are presented in Tab. 1. Convergence is reached in the majority of the angles when the mesh is refined until 60x60 elements.

2.6 Model Validation

The laminated plate that is used to validate the model is a square plate, made of Graphite-Epoxy and its properties are described in the Tab. 2.

The plate that is used to validate the model is simply supported in all the edges and the results after analysis is compared with Narita and Leissa results [8]. A compressive uniaxial load N_x is applied to opposite edges, and the critical load is obtained for distinct fibers angles. The four first rows of Tab. 3 shows the buckling parameter λ obtained in function of the variation of lamination angle - θ when the one ply laminated is analysed. The first row

Table 1. Convergence Mesh Test

	Critical Load [N/m]						
Mesh	0^o	15^o	30^o	45^o	60^o	75^o	90^o
15X15	44.82	44.19	43.71	43.74	40.46	29.67	25.70
30X30	44.79	44.30	44.06	44.20	40.51	29.72	25.74
45X45	44.79	44.35	44.22	44.41	40.59	29.77	25.77
60X60	44.80	44.39	44.31	44.54	40.67	29.80	25.77
75X75	44.80	44.39	44.36	44.54	40.67	29.80	25.77

Table 2. Composite Material Properties

Graphite-Epoxy AS 3501			
$E_1(GPa)$	$E_2(GPa)$	$G_{12}(GPa)$	ν_{12}
138.0	8.96	7.1	0.1

presents the θ angle in degrees. The second row of this table shows the results obtained by Narita and Leissa [8] using Ritz with Navier function, eq. (7), with $M, N = 10$ terms.

$$\sum_{m=1}^{M}\sum_{n=1}^{N} C_{mn} sin\frac{m\pi x}{a} sin\frac{m\pi y}{b} \tag{7}$$

The third row presents the λ obtained by this research using Finite Element Method, and the fourth row shows the difference between the parameter obtained by the reference [8] and this work. The fifth, sixth, seventh and eighth row presents the results and the difference between this research and the reference when the laminate has three layers $[\theta/-\theta/\theta]$. Similarly, the ninth, tenth, eleventh and twelfth row shows the results obtained by paper [8] and by this analysis considering a laminate with five layers $[\theta/-\theta/\theta/-\theta/\theta]$.

Table 3. Variation of Buckling Parameters - λ according to fiber angle for one ply - θ, three plies - $\theta/-\theta/\theta$ and five plies $\theta/-\theta/\theta/-\theta/\theta/$

θ	0^o	15^o	30^o	45^o	60^o	75^o	90^o
λ [8]	12.91	12.63	12.41	12.35	10.96	8.43	7.43
λ	12.91	12.39	11.36	10.83	10.20	8.21	7.43
Diff(%)	0.00	-1.92	-8.49	-12.34	-6.89	-2.61	0.00
$\theta/-\theta/\theta$	0^o	15^o	30^o	45^o	60^o	75^o	90^o
λ [8]	12.91	12.99	13.63	14.1	12.37	8.77	7.43
λ	12.91	12.79	12.77	12.83	11.71	8.58	7,43
Diff(%)	0.00	-1.56	-6.33	-8.99	-5.33	-2.11	0.00
$\theta/-\theta/\theta/-\theta/\theta$	0^o	15^o	30^o	45^o	60^o	75^o	90^o
λ [8]	12.91	14.21	17.11	18.66	16.49	9.94	7.43
λ	12.91	14.11	16.77	18.16	16.17	9.84	7,42
Diff(%)	0.00	-0.68	-2.01	-2.67	-1.94	-1.01	-0.08

Independent of the number of layers, the highest difference between the reference and this model is obtained when the angle is 45 degrees. The lowest difference occurs when the angle is 0 or 90 degrees. As shown in Tab. 3, when the number of layers increases, the difference decreases such that the highest difference is less than 3%. Thus, the results obtained by finite elements are more conservative than those obtained by Ritz because they are the smallest.

The results of Tab. 3 are plotted in Fig. 2 that presents the variation of buckling parameter in function of the lamination angle. In this figure is observed clearly the difference mainly when the fibers are 45 degrees with the axis. Besides this, it can be seen the decrease of the difference when the number of layers increases.

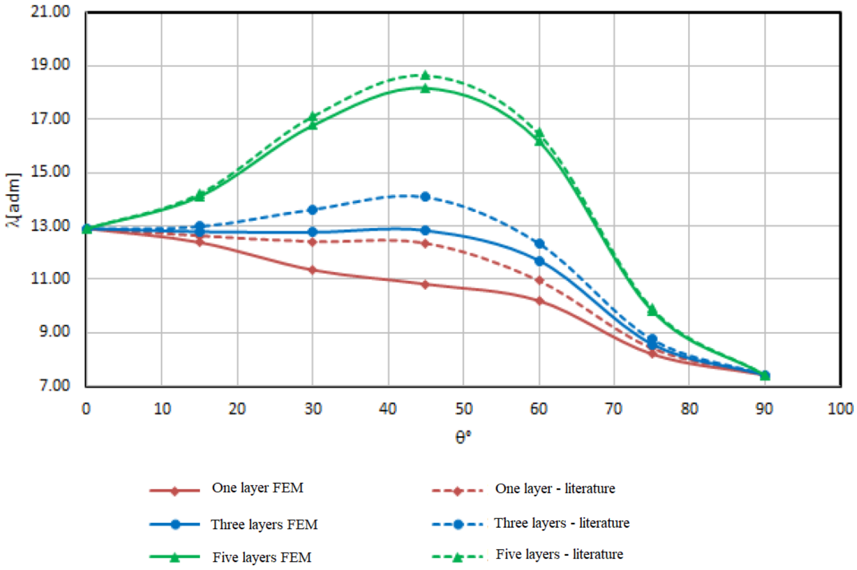

Figure 2. Laminated Simply Supported Plate Critical Load compared with [8]

3 Results and Discussions

The results presented here were obtained after analysis using finite elements, and the figures were plotted to square laminated plates changing the boundary conditions and the number of layers.

The Figure 3A shows the variation of the critical load of simply supported square plate when the lamination angle changes. The critical load is maximum when the lamination angle is 45 degrees and this figure also shows that after nine layers the maximum critical load does not change. When the lamination angle is 90 degrees the critical load reaches the minimum (36% in relation to the maximum) because the fibers are perpendicular to the uniaxial compressive load.

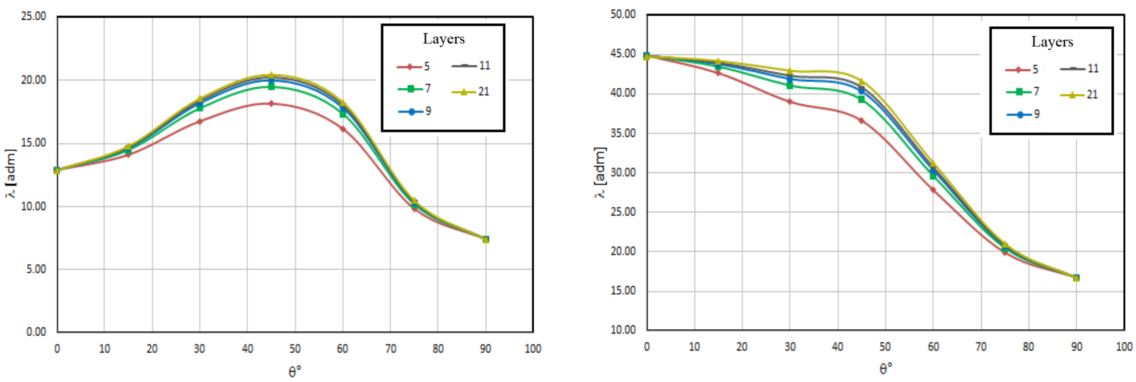

(A) Simply Supported Plate

(B) Laminated Clamped Plate

Figure 3. Laminated Simply Supported and Clamped Plate - Critical Load

Figure 3B shows that the maximum critical load is reached aligned to the compressive load (zero degrees) and the minimum is perpendicular when the edges are clamped (90 degrees). The greatest fall of the critical load is reached when the lamination angle is bigger than 45 degrees. The load critical difference between the number of layers is more detachable when the plate has five plies.

Figure 4 shows the behaviour of the plate with clamped and Simply Supported edges. The load is applied to the clamped edges. The critical load decreases as that lamination angle increases to 90 degrees. Furthermore, the influence of free edges can be observed in Fig. 5A that has simply supported and free edges and Fig. 5B that has clamped and free edges. The behaviour is the same independent of the number of layers, and the lowest critical load occurs when the lamination angle is 90 degrees.

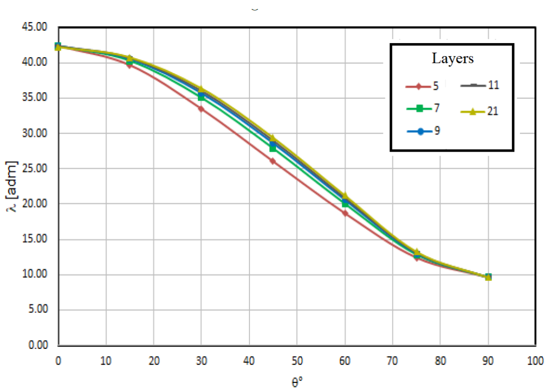

Figure 4. Laminated Plate with Clamped and Simply Supported Edges - Critical Load

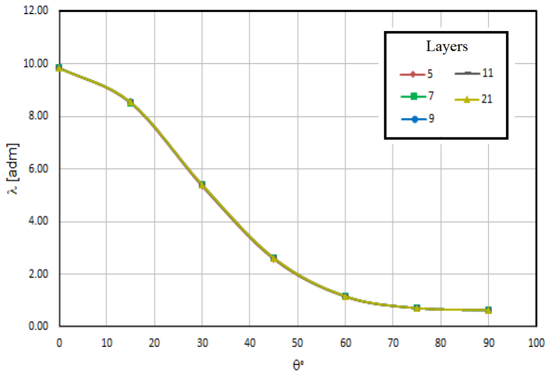

(A) Simply Supported and Free Edges

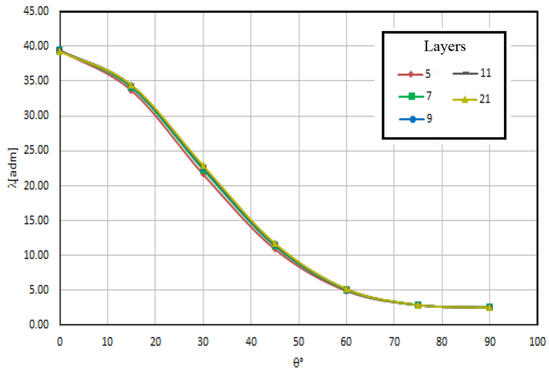

(B) Clamped and Free Edges

Figure 5. Laminated Plate - Critical Load

Figures 6A and 6B present the simply supported and clamped five layers laminated plate buckling modes, respectively. The figures show the modes varying according to lamination angle. The red color represents the maximum deflection and the magenta is the minimum deflection.

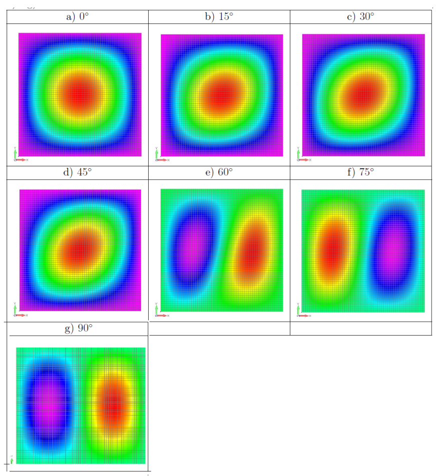

(A) Simply Supported Modes

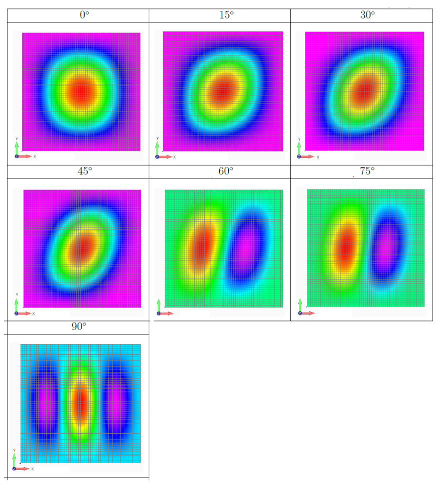

(B) Clamped Modes

Figure 6. Laminated Plate - Buckling Modes

4 Conclusions

Several analyses can be developed using the Finite Element Method, turning it possible to evaluate the influence of different boundary conditions, number of layers, and lamination angles in the plate buckling. As seen in the previous section, the results of the method are improved when the number of layers increases. Moreover, in simply supported plates, the maximum critical load is reached at 45 degrees, while in clamped plates the maximum is achieved at zero degrees. When the plate has two free edges, called the column plate, the maximum is also reached at zero degrees. In this case, the λ does not change when the number of layers increases, but the critical load, N_x in eq. (5), changes with thickness and the length of the plate.

Authorship statement. The authors hereby confirm that they are the sole liable persons responsible for the authorship of this work, and that all material that has been herein included as part of the present paper is either the property (and authorship) of the authors, or has the permission of the owners to be included here.

References

[1] T. S.P. and W.-K. S. *Theory of plates and shells*. Mac Graw Hill, New York,USA, 1959.
[2] U. A.C. *Stresses in plates and shells*. Mac Graw Hill, New York,USA, 1981.
[3] J. Reddy. *Theory and analysis of elastic plates and shells*. CRC Press, 2006.
[4] R. Jones. *Mechanics of Composite Materials*. Edward Brothers, Ann Arbor,MI,USA, 2nd ed. edition, 1999.
[5] C. Kassapoglou. *Design and Analysis of Composite Structures with Applications to Aerospace Structures*. John Wiley and Sons, West Sussex,UK, first ed. edition, 2010.
[6] J. Reddy. *Mechanics of Laminated Composite Plates and Shells Theory and Analysis*. CRC Press, Boca Ratton, Florida,USA, 2nd ed. edition, 1997.
[7] G. Staab. *Laminar Composites*. Elsevier, Waltham, Massachusetts,USA, 2nd ed. edition, 2015.
[8] Y. Narita and A. Leissa. Buckling studies for simply supported symmetrically laminated rectangular plates. *International Journal of Mechanical Sciences*, vol. 32, n. 11, pp. 909–924, 1990.
[9] Siemens. *NX Nastran User's Guide*. Siemens, 2016.